공학석사학위논문

폴리에틸렌글리콜을 개질한 프로피온산 셀룰로오스의 제조 및 분석과 고체 고분자 전해질로의 응용

Preparation and Characterization of Poly(ethylene glycol) Modified Cellulose Acetate Propionate and Its Application for Solid Polymer Electrolyte

2018년 2월

서울대학교 대학원

화학생물공학부

김 동 민

폴리에틸렌글리콜을 개질한 프로피온산 셀룰로오스의 제조 및 분석과 고체 고분자 전해질로의 응용

Preparation and Characterization of Poly(ethylene glycol) Modified Cellulose Acetate Propionate and Its Application for Solid Polymer Electrolyte

지도교수 이 종 찬

이 논문을 공학석사 학위논문으로 제출함.

2018년 2월

서울대학교 대학원

화학생물공학부

김 동 민

김동민의 공학석사학위논문을 인준함.

2018년 2월

위 원 장 _____(印)

부위원장 _____(印)

위　　원 _____(印)

Abstract

Preparation and Characterization of Poly(ethylene glycol) Modified Cellulose Acetate Propionate and Its Application for Solid Polymer Electrolyte

Dong Min Kim

Polymer Chemistry

Department of Chemical & Biological Engineering

Seoul National University

Cellulose acetate propionate was modified by esterification reaction with poly(ethylene glycol) using DCC/DMAP catalysts. The grafted poly(ethylene glycol) ratio in cellulose acetate propionate backbone were controlled by adjusting the amount of reactant. And the grafting yield could be quantitatively calculated using ^{1}H nuclear magnetic resonance. As grafting yield increased, poly(ethylene glycol) interfered with the interaction between cellulose acetate propionate

backbone, resulting in a decrease in the crystallinity and an increase in d-spacing value of cellulose acetate propionate. And due to the flexible poly(ethylene glycol) side-chain, glass transition temperature also decreased linearly with increasing grafting yield. Using the modified cellulose acetate propionate with different grafting yield, the homogeneous dimensionally-stable free-standing films used for solid polymer electrolyte were prepared. Compared with the glass transition temperature before the addition of Li cation, it increased when Li cation was added due to the interaction with poly(ethylene glycol) which could move the Li cation. As the grafting yield of the poly(ethylene glycol) conducting Li cation increased, the ionic conductivity of prepared films also increased.

Keywords: cellulose acetate propionate, poly(ethylene glycol), DCC/DMAP esterification, modification contents

Student Number: 2016-21007

List of Tables

List of Scheme

List of Figures

List of Contents

1. Introduction

Cellulose, which is the most abundant and renewable natural polymers, is a promising biodegradable, environment-friendly raw material with an excellent low cost.[1-3] Cellulose has been studied extensively for more than one hundred years, in order to reduce the petroleum-dependent materials and the environment pollution. However, due to the hydrogen bonding in its chain and hydrophilic nature of cellulose, it has poor solubility in common organic solvents, which limits the utilizations of cellulose.[4] Cellulose acetate propionate (CAP) is obtained by hydrolysis of cellulose using acetic acid and propionic acid.[5] The intermolecular binding force between CAP backbones is weakened by the substituted acetate and propionate groups instead of the hydroxyl group, and the hydrophilic properties of CAP are reduced, which is well soluble in common organic solvents. Because CAP obtained by processing cellulose also has the bio-degradable, abundant, renewable properties of cellulose, it has been applied to various fields. In many papers, CAP has been used as solid polymer electrolyte (SPE) of supercapacitor through acid

doping,[5] an additive to enhance the physical properties,[6, 7] membrane which was used for forward osmosis[8-10] or as an eco-friendly polymer film.[11, 12]

In recent years, concerns about the environment have driven research into the modification of bio-fibers.[13, 14] Because cellulose has three hydroxyl groups per anhydroglucose unit (AGU), these groups are mainly responsible for the various modification reactions of cellulose.[15] In many studies, the desired properties have been successfully introduced into cellulose and cellulose derivate through esterification reaction with carboxylic acid,[16] etherification reaction,[17] free radical graft polymerization reaction,[18] or ring-opening polymerization reaction.[19] Using these chemical reactions, existing petroleum-based materials could be replaced with environmentally friendly cellulose-based materials.

The biological and ion-conducting properties of poly(ethylene glycol) (PEG) and their biocompatibility have made these polymers useful for various fields.[20] Especially, in lithium-ion battery, PEG groups are an important functionality to transport Li cations. Due to its highly crystalline characteristic, it is not good for transporting Li cations. So grafting low molecular weight PEG to the polymer

chains, crystallinity of PEG could be suppressed. Due to grafted PEO chain and increasing flexibility of chains, Li cations could be successfully transported by bonding with the PEO.

In this study, the PEG groups were grafted onto the CAP which is cellulose derivate through N,N′-Dicyclohexylcarbodiimide (DCC), 4-(Dimethylamino)-pyridine (DMAP) coupling esterification reaction. DCC has been widely used for coupling agent because it promotes the esterification reaction in the mild condition.[20, 21] Also, when DMAP is added with DCC, the rate of esterification and yield increases.[22] The amount of grafted PEG was quantitatively analyzed by adjusting the amounts of PEG, DCC, and DMAP relative to CAP. The physical properties with different ratio of substituted hydroxyl groups were analyzed. Moreover, the films with LiTFSI were prepared and their ionic conductivities were measured to compare the conductivity according to PEG contents.

2. Experimental

2.1. Materials

Cellulose acetate propionate(CAP, average M_n = 75,000 g mol^{-1}, Sigma-Aldrich), Succinic anhydride(SA, Sigma-Aldrich), and Polyethylene Glycol Monomethyl Ether 400(mPEG, TCI) are used as received. N,N′-Dicyclohexylcarbodiimide(DCC, Sigma-Aldrich), Tetrabutylammonium bromide(TBAB, Sigma-Aldrich), 4-(Dimethylamino)pyridine(DMAP, Thermo Fisher), was dried under high vacuum at ambient temperature for 24 h and subsequently placed in an argon filled glove box. Tetrahydrofuran (THF) was freshly distilled from sodium/benzophenone under a nitrogen atmosphere. All other reagents and solvents were obtained from reliable commercial sources and used as received.

2.2. Functionalization of mPEG

α-Monocarboxy-ω-monomethoxy poly(ethylene glycol), FmPEG was prepared by reacting Polyethylene Glycol Monomethyl Ether 400(mPEG) with succinic anhydride(SA) in the presence of a catalytic amount of TBAB. mPEG (MW=400, 12 g, 30 mmol), succinic anhydride (3.6 g, 36 mmol) and TBAB (0.172g 0.532mmol) were dissolved in 30ml of THF and stirred for 24 h at 80 ºC. The solvent was evaporated with a rotary evaporator. After filtration, the residue was diluted with methylene chloride(MC) and washed with 1 N hydrochloric acid aqueous solution in order to eliminate unreacted succinic anhydride. The organic layer was dried over anhydrous magnesium sulfate and concentrated under reduced pressure. The residue was dried in vacuo overnight. Yellow liquid was obtained.

^{1}H NMR (300 MHz, $CDCl_3$, δ (ppm), tetramethylsilane (TMS) ref): 4.23 (2H, C(O)O-CH_2-CH_2), 3.63 (4H, O-CH_2-CH_2), 3.53 (2H, C(O)O-CH_2-CH_2-O), 3.36 (3H, OCH_3), 2.63 (4H,CO-CH_2-CH_2-CO).

2.3. Esterification reaction between FmPEG and CAP

Cellulose acetate propionate-*g*-poly(ethylene glycol) (CP) was synthesized via esterification through DCC, DMAP coupling reaction as follows. CAP (2 g, 2.24 mmol) was completely dissolved in 60 ml distilled THF. Then FmPEG, DCC, and DMAP in the amount of Table 1 were slowly added into the above solution and reacted at 80 ºC for 24 h. The reaction byproduct diclyclohexylcarbodiurea (DCU) was removed by filtration and unreacted FmPEG, DCC and DMAP were removed by precipitation in excess amount of isopropyl alcohol(IPA)/hexane (v/v = 1) solvent. The obtained Cellulose acetate propionate-*g*-poly(ethylene glycol) (CP) was freeze-dried overnight.

^{1}H NMR (300 MHz, $CDCl_3$, δ (ppm), tetramethylsilane (TMS) ref): 3.4 – 5.1 (Cellulose acetate propionate backbone and PEG side-chains), 3.38 (3H, OCH_3), 2.0 – 2.5 (2H, CO-CH_2-CH_3), 0.9 – 1.3 (3H, CO-CH_2-CH_3).

Table 1. Amount of reactant, DS_{FmPEG}, Y_{graft}, and glass transition temperature of CP#

	FmPEG[a]	DCC[a]	DMAP[a]	DS_{FmPEG}[b]	Y_{graft}[b]	T_g (°C)[c]
CAP	-	-	-	-	0/54	140.0
CP15	2	1	0.25	0.10	15/54	105.4
CP22	3	3	0.75	0.14	22/54	89.6
CP28	3	4	1	0.18	28/54	75.0
CP38	4	3	0.75	0.25	38/54	64.7
CP44	5	5	1.25	0.29	44/54	52.6

[a] Molar ratio to CAP

[b] Calculated by ^{1}H NMR integral ratio

[c] Calculated by DSC thermograms

2.4. Preparation of solid polymer electrolytes (SPEs)

The solid polymer electrolytes containing LiTFSI and polymers in various blend compositions were prepared by a solution casting technique. Doping levels are defined as the ratio of the number of lithium cations (Li^+) to that of ethylene oxide (EO) repeating unit in the polymers ([Li]/[EO]). 0.1 g of polymers and the given amounts of LiTFSI ([Li^+] / [EO] = 0.07) were dissolved in 2 ml of THF and homogeneous solution was obtained. After that, the solution was cast onto a Teflon plate (2 x 2 cm^2) and dried at room temperature for overnight. Subsequently, it was further dried under high vacuum at room temperature for 24 h. Finally, the film was peeled off from the Teflon plate and the resultant film was placed in a high vacuum condition for a week at 80 ^oC prior to measure the ionic conductivities of the solid polymer electrolytes. The thickness of the films measured by a micrometer (Mitutoyo, 293-330 IP 65 water resistant) was in the range of 30-100 μm.

2.5. Characterization

^{1}H nuclear magnetic resonance (NMR) spectra were recorded on an Ascend^{TM} 400 spectrometer (300 MHz) using $CDCl_3$ (Cambridge Isotope Laboratories) as the solvent at room temperature with tetramethylsilane (TMS) as a reference. Attenuated total reflectance Fourier transform infrared (ATR FT-IR) spectroscopy was performed on a Jasco FT-IR 200 in the wavenumber range from 4000 to 650 cm^{-1} with a resolution of 4 cm^{-1}. X-ray diffraction (XRD) patterns were acquired with RI-GAKU MODE 1 SMARTLAB using a monochromatic CuKα (1.5406 Å) radiation. The thermal transition temperatures of the polymers were examined by differential scanning calorimetry (DSC) using TA Instruments DSC-Q1000 under a nitrogen atmosphere. Samples with a typical mass of 3-7 mg were encapsulated in sealed aluminum pans. The samples were first heated to 250 ºC and then quenched to 0 ºC. This was followed by a second heating scan from 0 ºC to 250 ºC at a heating rate of 10 ºC min^{-1}. The ionic conductivity of the SPEs was analyzed by complex impedance spectroscopy between 10 to 80 ºC under dry nitrogen condition using

Zahner Electrik IM6 apparatus in the frequency range of 0.1 Hz to 1 MHz and an applied voltage of 10 mV. The real part of the impedance at the minimum of imaginary part was used as the resistance to calculate the conductivity of the SPEs. The samples for the measurements were prepared by sandwiching the SPEs between two stainless-steel electrodes. Each sample was allowed to equilibrate for 30 min at each temperature prior to taking measurements. The ionic conductivity (σ) was calculated from the electrolyte resistance (R) obtained from the impedance spectrum, the electrolyte thickness (d) and the area of the electrode (A) using the following equation, $\sigma = (1/R) \times (d/A)$.

3. Result and Discussion

3.1. Characterization of functionalized mPEG (FmPEG)

α-Monocarboxy-ω-monomethoxy poly(ethylene glycol) (FmPEG) was synthesized via reaction between poly(ethylene glycol) monomethyl ether (mPEG) and succinic anhydride(SA) using tetrabutyl ammonium bromide (TBAB) as an catalyst (Scheme 1). TBAB is a catalyst for promoting esterification and is easy to purify because it is well soluble in water.[23, 24]

Figure 1 showed the ^{1}H-NMR data of FmPEG and CP. According to figure 1, peak “d” (3.71 ppm) was shifted to peak “f” (4.23 ppm) and a new peak “e” (2.63 ppm) appeared. The peaks e and f corresponded to four protons of -COC*H*$_2$C*H*$_2$-COOH and two protons of -COOC*H*$_2$CH2O, respectively. The yield was obtained by using the integration area ratio between peak “a” at 3.36 ppm to peak “f” at 4.23 ppm, and the yield obtained was 97%. This is obvious evidence that most of the

Scheme 1. Synthesis of cellulose acetate propionate-*graft*-poly(ethylene glycol) (CP).

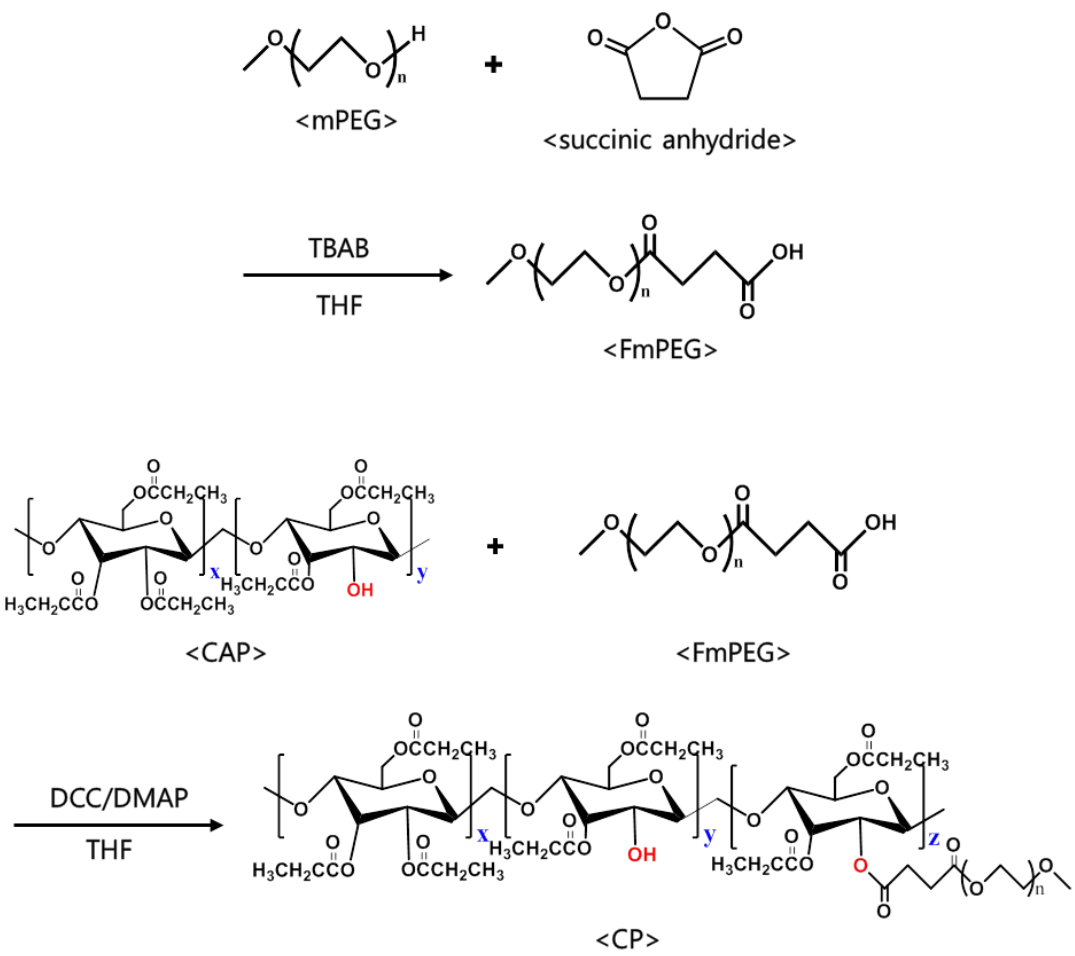

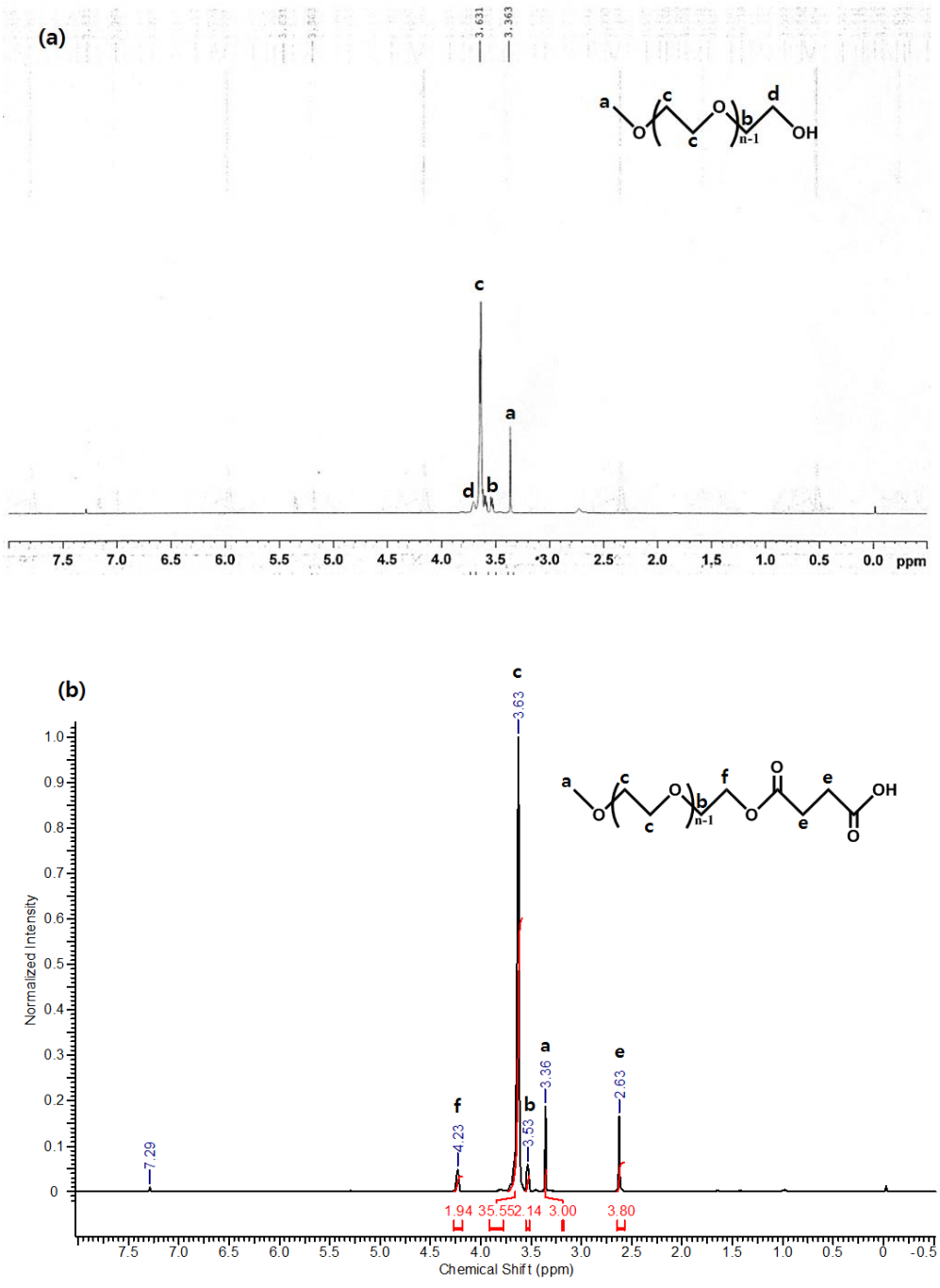

Figure 1. ^{1}H NMR Spectra of mPEG (a), FmPEG (b).

monohydroxyl end groups of the mPEG were successfully substituted with succinic anhydride.

3.2. Synthesis of CP# and structural analysis

Cellulose acetate propionate(CAP) is a randomly grafted polymer of propionyl and acetyl groups on the backbone. The ratio of the propionyl group to the acetyl group of the CAP backbone could be determined using ^{13}C-NMR.[25, 26] The propionyl and acetyl groups were observed as triplet at about 173 ppm and 170 ppm, respectively.[27] According to Figure 2, only propionyl group existed in CAP. Also, the ratio of the OH functionality on CAP backbone could be obtained through as integral ratio of ^{1}H-NMR. The peaks “c” (3.5-5.3 ppm) and “a” (1.09, 1.21 ppm) corresponded to seven protons of CAP backbone and three protons of –OCOCH$_2$C*H$_3$* of propionyl group, respectively. Therefore, the ratio of x and y could be obtained by using the following equation.

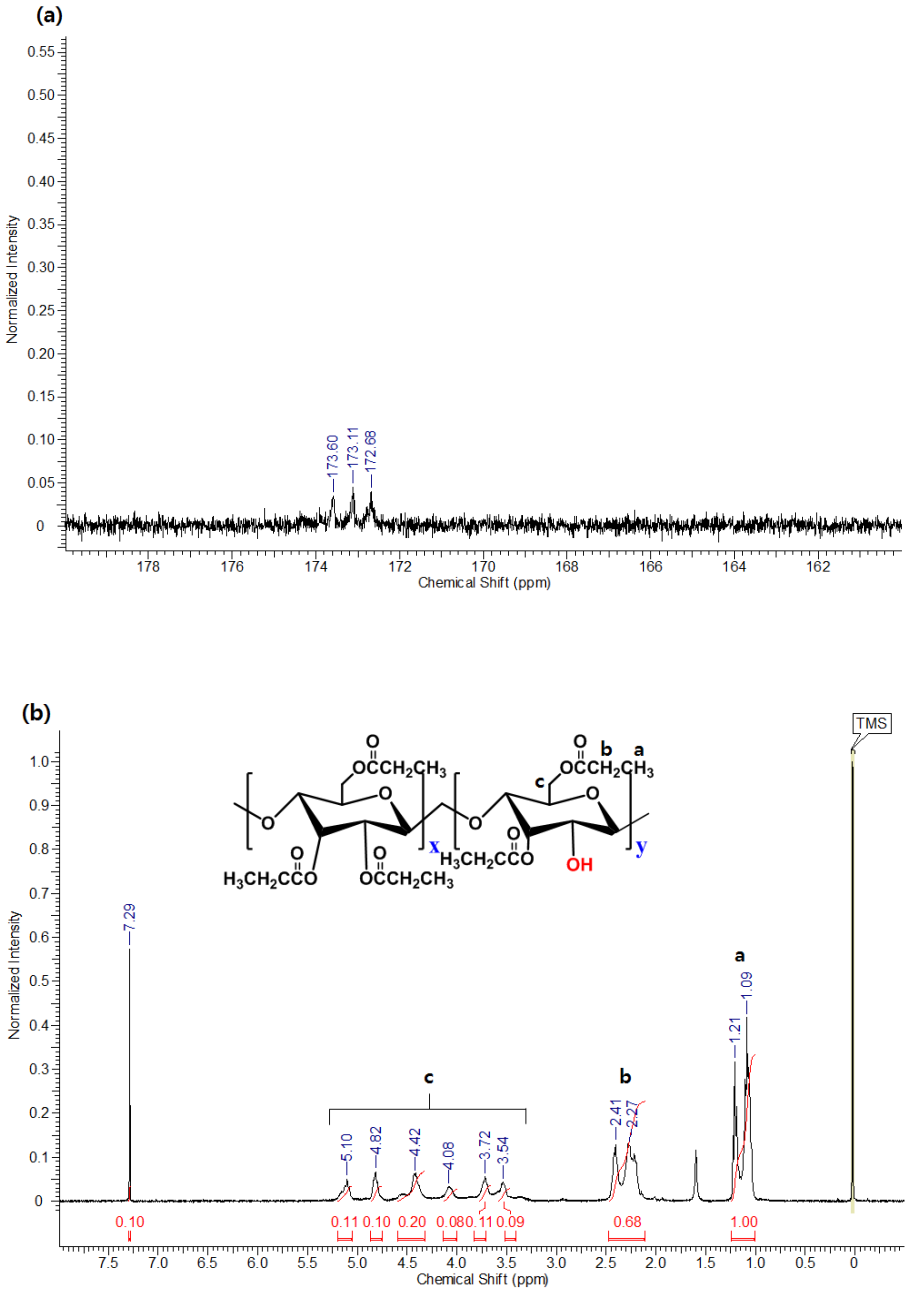

Figure 2. ^{13}C NMR (a) and ^{1}H NMR (b) Spectra of CAP.

$$\frac{I_a/3}{I_c/7} = \mathrm{DS_{CAP}}$$

Where I_a and I_c are the integrated intensities of a, c proton peaks in Figure 2(b), respectively. $\mathrm{DS_{CAP}}$ (degree of substitution of CAP) is the number of propionyl groups per anhydroglucose unit (AGU) of CAP.

$$3x + 2y = \mathrm{DS_{CAP}}(x + y)$$

Where x means the proportion of AGU with three propionyl groups, and y means the proportion of AGU with one hydroxyl and two propionyl groups.

The $\mathrm{DS_{CAP}}$ was 2.65 and calculated ratio $\mathrm{x : y} = 100 : 54$. The remaining OH functionality on CAP chains can be used to introduce other functionalities

through conventional organic reactions, such as an esterification. In this study, cellulose acetate propionate-*graft*-poly(ethylene glycol) (CP) was synthesized by coupling reaction of FmPEG to CAP in the presence of DCC as coupling agent and DMAP as catalyst (Scheme 1).[22] To control grafting yield (Y_{graft}), the amounts of FmPEG, DCC, and DMAP were varied as shown in Table 1. Y_{graft} is the ratio of grafted FmPEG to total hydroxyl groups before reaction. CP with different Y_{graft} are abbreviated as CP#, where # indicates the amount of FmPEG substituted when the total hydroxyl groups are taken as 54. Representative ^{1}H NMR spectrums of CP# were shown in Figure 3, which is compared with the precursor CAP as shown in Figure 2(b). In Figure 3(a), the proton peak observed at 3.38 ppm was clearly assigned to methyl proton of FmPEG in CP15. Similarly, a methyl proton peak of FmPEG was also observed in CP#. These peaks indicate the presence of FmPEG units in the polymers. The degree of FmPEG substitution (DS_{FmPEG}) can be estimated by the ^{1}H NMR spectra using following equation.[28]

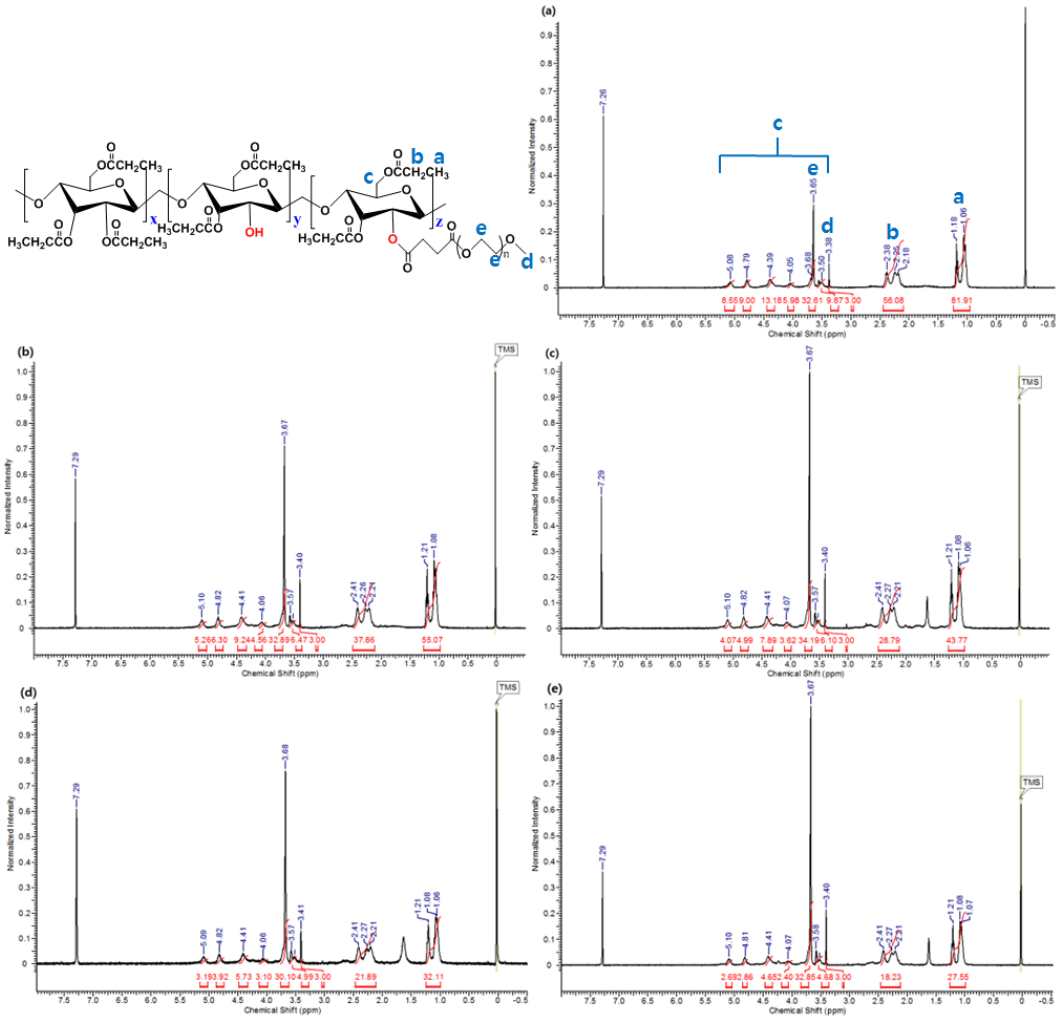

Figure 3. ^{1}H NMR Spectra of CP15 (a), CP22 (b), CP28 (c), CP38 (d), CP44 (e).

$$DS_{FmPEG} = \frac{I_d}{I_a} \times DS_{CAP}$$

Where DS_{FmPEG} is the number of FmPEG groups per anhydroglucose unit (AGU) of CAP.

$$3x + 2y + 2z = DS_{CAP}(x + y + z)$$

$$z = DS_{FmPEG}(x + y + z)$$

Where z means the proportion of AGU with one FmPEG and two propionyl groups.

Table 1 shows DS_{FmPEG} and Y_{graft} of CP# calculated by ^1H NMR. As FmPEG, DCC, and DMAP increased, DS_{FmPEG} and Y_{graft} increased.

3.3. Analysis of CP#

The incorporation of FmPEG into the CAP was further confirmed by IR spectroscopy as shown in Figure 4. Because of the carbonyl groups (C=O) observed near 1700 cm^{-1} and the absence of hydroxyl group observed near 3500cm^{-1} in FmPEG, monohydroxyl group in mPEG was successfully substituted with succinic anhydride. As the Y_{graft} of CP# increased, the hydroxyl group which was located at 3491 cm^{-1} decreased. The OH functionality in CAP backbone was successfully reduced by the esterification reaction. Also, absorbance intensities of the peak 2881 cm^{-1} gradually increased as FmPEG proportion in CP# increased, because sp3 C-H stretching region in FmPEG is located in 2868 cm^{-1}. In Figure 4(b), C-O-C stretching regions at 1094 cm^{-1} and 1033cm^{-1} appeared in FmPEG.[29, 30] Due to the strong C-O-C stretching peaks in grafted FmPEG side chains, peak intensities at 1081 cm^{-1} and 1033cm^{-1} of CP# gradually increased.

Figure 5(a) shows the XRD patterns of CAP and CP#. Based on the XRD

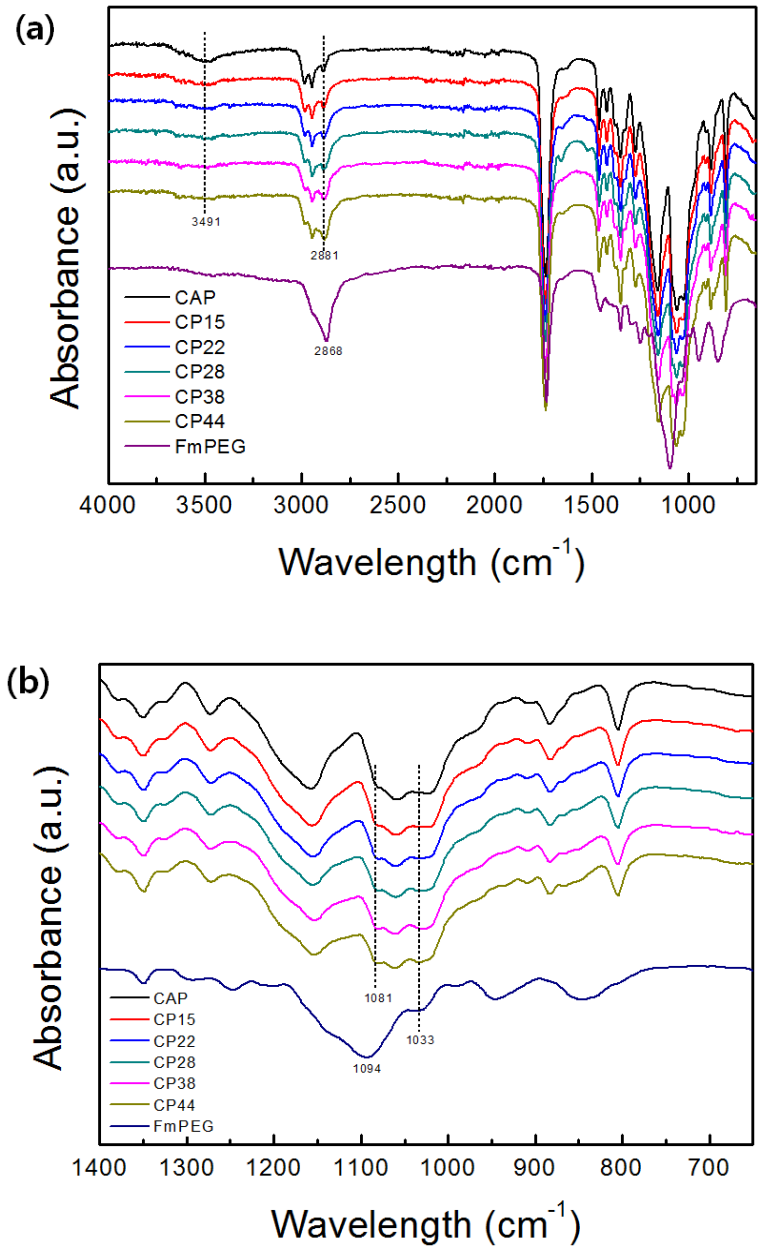

Figure 4. FT-IR spectra of CP# and FmPEG in the frequency range 4000-650 cm^{-1} (a) and 1400-650 cm^{-1} (b).

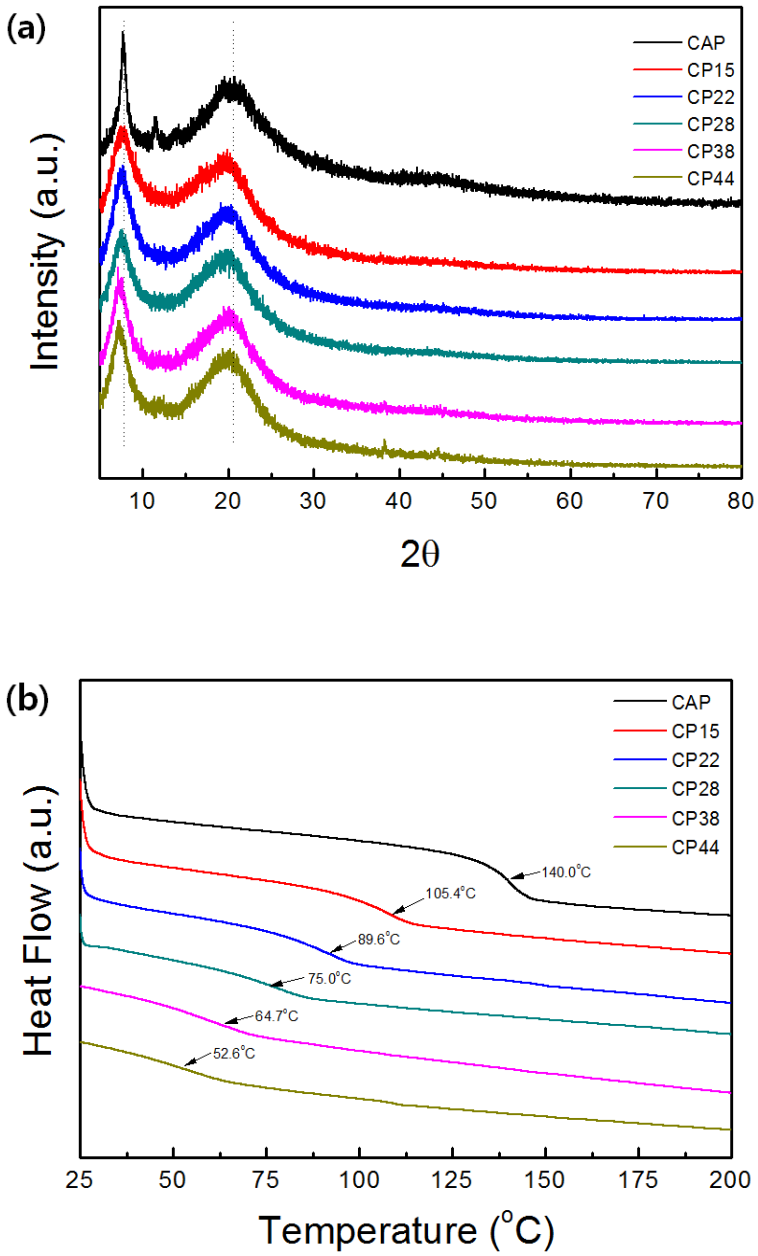

Figure 5. XRD patterns (a) and DSC thermograms (b) of CAP and CP#.

pattern of CAP, the appearance of diffraction peaks at 7.7º, 11.6 º, 20.5 º shows the typical characteristic of crystalline peaks of CAP. As the amount of substituted FmPEG increased, the peak at 7.7º became more broadened and shifted to left side. The d-spacing values could be calculated through the 2θ value of XRD by the following equation.[31]

$$\lambda = 2d\sin\theta$$

Where λ is a device specific value, 1.5406 Å.

The 2θ value of CAP was 7.7º, and the corresponding d-spacing value was 1.15 nm. After the esterification reaction, the 2θ value of CP44 was shifted to 7.3º and the d-spacing value increased to 1.21 nm. Because of grafted FmPEG onto the CAP backbone, the crystalline characteristic of the CAP decreased and

the spacing between backbone chains increased.

The thermal properties of the CAP and CP# based on DSC measurements are shown in Figure 5(b). The glass transition temperature (T_g) of samples are summarized in Table 1. Before reaction, the T_g value of CAP was 140.0 ^oC.[32, 33] As the amount of substituted FmPEG increased, the T_g values of CP# decreased. As shown in Figure 5(a), the grafted FmPEG increased the d-spacing between the CAP backbones. Also, introduction of FmPEG which has flexible properties due to $–OCH_2CH_2O-$ units leads to an increment of the free volume of the polymer chains.[34, 35] Therefore, CAP chain segment moved more easily and fraction of amorphous region increased. The reduction of crystallinity resulted in a T_g drop.

3.4. Preparation of solid polymer electrolytes (SPEs)

The solid polymer electrolytes containing LiTFSI and polymers were prepared by a solution casting technique. Typically, in order to prepare free-standing SPEs,

UV was treated with cross-linking agents[36, 37], semi-interpenetrating network was introduced[38], or additives were added[39]. In this paper, because of high molecular weight polymer, homogeneous free-standing films were prepared without additives. The molar ratio of Li^+ to ethylene oxide (EO) was fixed at 0.07 as shown in Table 2, because the highest ionic conductivity was obtained at this concentration.[37] After casting CP# and LiTFSI solution dissolved in THF, the solvent was dried overnight, and then homogeneous films (CP# film) were obtained.

Figure 6(a) shows the XRD patterns of CAP and CP# film. The major diffraction peaks for CAP film appeared at 7.8º, 11.4º, 20.5º. Compared with Figure 5(a), the addition of LiTFSI showed no significant change in the crystalline properties of CAP. And as FmPEG was grafted to CAP, the peaks were broadened and shifted to the left. The d-spacing values of films could be calculated in the same way as above. The 2θ values of CAP film were 7.7º and 20.5º, and the corresponding d-spacing values were 1.15 nm and 0.43 nm. After esterification reaction, the 2θ values of CP44 film were shifted to 7.3 and 19.3, and the d-

Table 2. Amount of LiTFSI, T_g, and Ionic conductivity of CP# film

	LiTFSI (wt%)	$[Li^{+}]$ / [EO]	T_g (°C)[a]	Ionic conductivity (at 80 °C)
CAP film	4.3[b]	-[b]	139.8	-
CP15 film	4.3	0.07	122.5	1.2×10^{-9} S/cm
CP22 film	6.0	0.07	90.5	5.8×10^{-9} S/cm
CP28 film	7.1	0.07	81.9	2.2×10^{-8} S/cm
CP38 film	8.8	0.07	74.5	1.4×10^{-7} S/cm
CP44 film	9.7	0.07	62.1	7.1×10^{-7} S/cm

[a] Measured with LiTFSI added film

[b] Same amount of LiTFSI with CP15 film

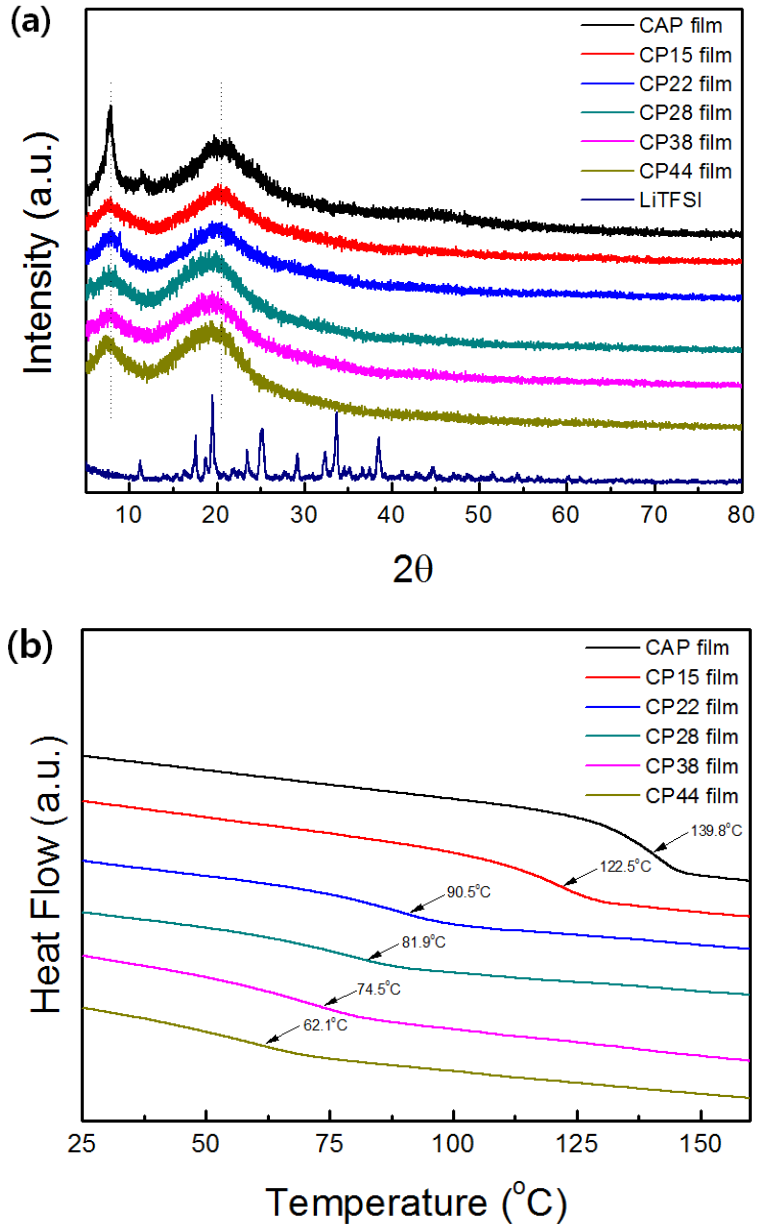

Figure 6. XRD patterns (a) and DSC thermograms (b) of CAP film and CP# films.

spacing values increased to 1.21 nm and 0.46 nm. Even when LiTFSI was added, the crystalline characteristic of the CAP film decreased and the spacing between backbone chains increased as FmPEG was grafted to CAP.

In Figure 6(b), the thermal transition behavior of the CAP and CP# films was investigated by DSC. The glass transition temperature (T_g) of films are summarized in Table 2. Before esterification reaction, The T_g value of CAP film was 139.8 ºC. There is no significant change in the T_g value compared with before adding LiTFSI. Comparing with XRD data of CAP and CAP film in Figure 5(a) and Figure 5(b), Li salts also did not affect crystallinity of CAP chains. As FmPEG was grafted to the CAP chains, T_g of CP# films with LiTFSI decreased gradually as did the CP# trend. Also, comparing the T_g values of the CP# samples, the T_g values of the CP# films were all increased. Lithium cations interfered with the flexibility of CP# through bonding with the oxygen atoms of PEO[36, 40]. Because of these interactions, chain mobility of CAP chains decreased and T_g increased.

3.5. Ionic conductivities of CP# films

Figure 7 shows temperature dependence of ionic conductivities of CP# films. The ionic conductivity is proportional to the number of charge carriers and the mobility of the charge carriers as follows

$$\sigma = \sum(n\ q\ \mu).$$

Where σ is the ionic conductivity, n is the number of charge carriers, q is the charge on the charge carrier, and μ is the mobility of the charge carrier.[41] As shown in Figure 6(a) and 6(b), grafting of FmPEG resulted in a decrease of crystallinity and increase of d-spacing between CAP chains. Along with the lithium cations transfer capability of PEO, ion conductivities increased as FmPEG grafted. Ionic conductivity increased linearly with increasing temperature in CP#

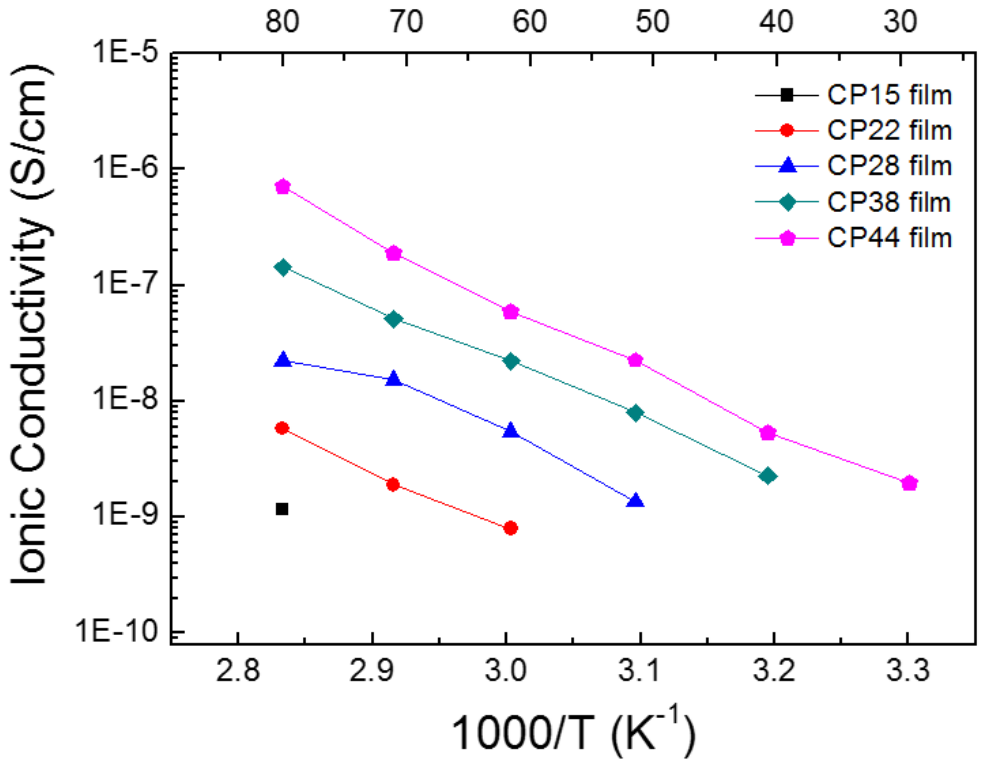

Figure 7. Temperature dependence of ionic conductivities of CP# films.

film, but was not measured for CAP film. Ionic conductivities at 80ºC were summarized in Table 2. Due to the crystallinity and high T_g of CAP, ion conductivity was not measured at all temperatures. Ion conductivities increased as grafting of FmPEG, which could transport Li cations to the CAP backbone. When the conductivities at 80ºC were compared, the conductivity of the CP15 film was about 600 times higher than that of CP44 film.

4. Conclusion

In this study, the structure was quantitatively analyzed by ^{1}H-NMR and ^{13}C-NMR, and FmPEG was grafted to CAP chain through coupling esterification reaction of DCC and DMAP. The amount of FmPEG grafted quantitatively was calculated by ^{1}H-NMR analysis of CP# samples. FT-IR analysis showed that the intensity of the hydroxyl group was decreased and the peak of FmPEG was increased. XRD patterns showed that the grafting of FmPEG increased the d-spacing of the CAP chain from 1.15 nm to 1.21 nm, and DSC showed that the T_g values decreased gradually from 140 ºC to 52.6 ºC. Also, XRD and DSC were measured by adding LiTFSI to the CP# samples. Even with the addition of LiTFSI, the tendency of increasing d-spacing and decreasing T_g was maintained. T_g was higher in CP# films than the CP# due to the bonding between Li cations and oxygen atoms of PEO. Because of this tendency, the ionic conductivity of CP15 film at 80 ºC (1.2×10^{-9} S/cm) was increased 600 times to the conductivity

of CP44 film at 80 ºC (7.1 x 10^{-7} S/cm).

5. References

1. L. Brinchi, F. Cotana, E. Fortunati and J. M. Kenny, *Carbohydrate Polymers*, 2013, **94**, 154-169.
2. A. N. Frone, S. Berlioz, J.-F. Chailan and D. M. Panaitescu, *Carbohydrate Polymers*, 2013, **91**, 377-384.
3. Y. Yin, X. Tian, X. Jiang, H. Wang and W. Gao, *Carbohydrate Polymers*, 2016, **142**, 206-212.
4. C. Zhang, R. Liu, J. Xiang, H. Kang, Z. Liu and Y. Huang, *The Journal of Physical Chemistry B*, 2014, **118**, 9507-9514.
5. Y. N. Sudhakar, D. Krishna Bhat and M. Selvakumar, *Polymer Engineering & Science*, 2016, **56**, 196-203.
6. G. W. Jeon, J. E. An and Y. G. Jeong, *Composites Part B: Engineering*, 2012, **43**, 3412-3418.
7. R. J. Moon, A. Martini, J. Nairn, J. Simonsen and J. Youngblood, *Chemical Society Reviews*, 2011, **40**, 3941-3994.
8. P. Lu, Y. Gao, A. Umar, T. Zhou, J. Wang, Z. Zhang, L. Huang and Q. Wang, *Science of Advanced Materials*, 2015, **7**, 2182-2192.
9. J. Su, T. S. Chung, B. J. Helmer and J. S. de Wit, *Desalination*, 2013, **313**, 156-165.
10. J. Su, R. C. Ong, P. Wang, T. S. Chung, B. J. Helmer and J. S. De Wit, *AIChE Journal*, 2013, **59**, 1245-1254.
11. N. Y. Liang, T. M. Don, C. Y. Huang and W. Y. Chiu, *Journal of Applied Polymer Science*, 2017, **134**.
12. M. Do Socorro Rocha Bastos, L. Da Silva Laurentino, K. M. Canuto, L. G. Mendes, C. M. Martins, S. M. F. Silva, R. F. Furtado, S. Kim, A. Biswas and H. N. Cheng, *Polymer Testing*, 2016, **49**, 156-161.
13. S. C. Fox, B. Li, D. Xu and K. J. Edgar, *Biomacromolecules*, 2011, **12**, 1956-1972.
14. L. Wei and A. McDonald, *Materials*, 2016, **9**, 303.
15. D. Roy, M. Semsarilar, J. T. Guthrie and S. Perrier, *Chemical Society Reviews*, 2009, **38**, 2046-2064.
16. P. Månsson and L. Westfelt, *Journal of Polymer Science: Polymer Chemistry*

Edition, 1981, **19**, 1509-1515.

17. T. T. T. Ho, T. Zimmermann, R. Hauert and W. Caseri, *Cellulose*, 2011, **18**, 1391-1406.
18. K. Littunen, U. Hippi, L.-S. Johansson, M. Österberg, T. Tammelin, J. Laine and J. Seppälä, *Carbohydrate Polymers*, 2011, **84**, 1039-1047.
19. A. Carlmark, E. Larsson and E. Malmström, *European Polymer Journal*, 2012, **48**, 1646-1659.
20. S. Zalipsky, C. Gilon and A. Zilkha, *Journal of Macromolecular Science: Part A - Chemistry*, 1984, **21**, 839-845.
21. F. E. Ziegler and G. D. Berger, *Synthetic Communications*, 1979, **9**, 539-543.
22. B. Neises and W. Steglich, *Angewandte Chemie International Edition in English*, 1978, **17**, 522-524.
23. S. Feng and C. Li, *J. Agric. Food Chem.*, 2015, **63**, 5732-5739.
24. R. Ray, R. D. Jana, M. Bhadra, D. Maiti and G. K. Lahiri, *Chemistry – A European Journal*, 2014, **20**, 15618-15624.
25. C. Vaca-Garcia, M. E. Borredon and A. Gaseta, *Cellulose*, 2001, **8**, 225-231.
26. H. Kono, H. Hashimoto and Y. Shimizu, *Carbohydrate Polymers*, 2015, **118**, 91-100.
27. Y. Tezuka and Y. Tsuchiya, *Carbohydrate Research*, 1995, **273**, 83-91.
28. T. Hu, J. Yi, J. Xiao and H. Zhang, *Polymer journal*, 2010, **42**, 752.
29. W. Wieczorek, D. Raducha, A. Zalewska and J. R. Stevens, *The Journal of Physical Chemistry B*, 1998, **102**, 8725-8731.
30. I. Pucić and T. Jurkin, *Radiation Physics and Chemistry*, 2012, **81**, 1426-1429.
31. D. Zhao, F. Yang, Y. Dai, F. Tao, Y. Shen, W. Duan, X. Zhou, H. Ma, L. Tang and J. Li, *Carbohydrate Polymers*, 2017, **174**, 146-153.
32. E. S. Carvalho, R. J. Sánchez, M. I. B. Tavares and Á. C. Lamônica, *Journal of Polymers and the Environment*, 2010, **18**, 661-667.
33. K. Sugimura, Y. Teramoto and Y. Nishio, *Carbohydrate Polymers*, 2013, **98**, 532-541.
34. F.-J. Wang, Y.-Y. Yang, X.-Z. Zhang, X. Zhu, T.-s. Chung and S. Moochhala, *Materials Science and Engineering: C*, 2002, **20**, 93-100.
35. R. Wang, H. Mei, W. Ren and Y. Zhang, *RSC Advances*, 2016, **6**, 107021-107028.

36. J.-H. Baik, D.-G. Kim, J. Shim, J. H. Lee, Y.-S. Choi and J.-C. Lee, *Polymer*, 2016, **99**, 704-712.
37. J. Shim, L. Kim, H. J. Kim, D. Jeong, J. H. Lee and J.-C. Lee, *Polymer*, 2017, **122**, 222-231.
38. S.-J. Kwon, D.-G. Kim, J. Shim, J. H. Lee, J.-H. Baik and J.-C. Lee, *Polymer*, 2014, **55**, 2799-2808.
39. D.-G. Kim, J. Shim, J. H. Lee, S.-J. Kwon, J.-H. Baik and J.-C. Lee, *Polymer*, 2013, **54**, 5812-5820.
40. M. Watanabe, Y. Suzuki and A. Nishimoto, *Electrochimica Acta*, 2000, **45**, 1187-1192.
41. H.-Y. Wu, D. Saikia, C.-P. Lin, F.-S. Wu, G. T. K. Fey and H.-M. Kao, *Polymer*, 2010, **51**, 4351-4361.

국문 요약

커플링제인 DCC와 촉매 DMAP을 사용하여 폴리에틸렌글리콜과 프로피온산 셀룰로오스의 에스터화 반응을 진행하였다. 반응물의 양을 조절하며 프로피온산 셀룰로오스 주쇄에 개질된 폴리에틸렌글리콜의 양을 조절하였다. 또한 개질된 폴리에틸렌글리콜의 양을 ^{1}H-NMR을 이용하여 정량적으로 분석하였다. 개질 함량이 증가함에 따라 결정성이 감소하며, 주쇄간의 거리가 증가하였다. 또한 유연한 폴리에틸렌글리콜 측쇄의 도입으로 유리전이온도가 감소하였다. 폴리에틸렌글리콜으로 개질한 프로피온산 셀룰로오스를 고체 고분자 전해질으로 제조하였다. 리튬 이온이 첨가됨에 따라 폴리에틸렌글리콜과 리튬 이온의 상호작용으로 유리전이온도가 상승하였으며, 이온전도도가 증가하였다.

주요어: 프로피온산 셀룰로오스, 폴리에틸렌글리콜, DCC/DMAP 에스터화 반응, 개질 함량 조절

학번: 2016-21007